



Photo-Stimulable Phosphor Plate Imaging Systems and Ambient Light Exposure: Effect of Timing on Quantitative Image Quality Tests

Hakan Amasya^{1,2,3} 

¹Department of Oral and Dentomaxillofacial Radiology, İstanbul University-Cerrahpaşa, Faculty of Dentistry, İstanbul, Türkiye

²CAST (Cerrahpaşa Research, Simulation and Design Laboratory), İstanbul University-Cerrahpaşa, İstanbul, Türkiye

³Health Biotechnology Joint Research and Application Center of Excellence, İstanbul, Türkiye

Cite this article as: H. Amasya, "Photo-stimulable phosphor plate imaging systems and ambient light exposure: effect of timing on quantitative image quality tests," *Electrica*, 25, 0116, 2025. doi: 10.5152/electrica.2025.24116.

ABSTRACT

Photo-stimulable phosphor imaging systems can be used in daylight, but the energy stored in the plate fades with ambient light and delay. In this study, an Arduino-based experimental platform was revised to generate continuous and interrupted light. Scanning of the plates was delayed for a total of 4 minutes, while light was emitted for a total of 2 minutes. In continuous experiments, the light was applied at the beginning, middle, and end of the period, while in interrupted experiments, the light was switched on and off at a ratio of 1:3 at different time intervals. Half of the plates were protected from the ambient light during exposure. Signal-to-noise (SNR) and Contrast-to-noise (CNR) ratios were calculated using the second and fourth regions of the step-wedge. On the light side, the highest SNR values were found in the 5–15 s and the lowest in the 250–750 ms interrupted sequences. Contrast-to-noise values ranged between 23.7 and 46.7. On the dark side, the highest SNR value was found in the 250–750 ms experiment, while the lowest was calculated in the continuous light experiment with the middle sequence. Contrast-to-noise values were found between 76.6 and 154.6. The mean SNR values were higher on the light side, while the mean CNR values were lower ($p=0.02$). This may indicate that the image correction algorithm results in a gain in SNR and a loss in CNR. The tool used in this research is different from other studies in terms of the modulation of LEDs and sensor tracking, and it is the first among the experiments conducted with the box by investigating the effect of different timings in the same color. This research is aimed at obtaining results in the sense of materials science, rather than an outcome that will be used directly in the clinic.

Index Terms— Additive manufacturing, Arduino, dental, developer board, photo-stimulable phosphor plates, radiology

I. INTRODUCTION

Microcontrollers (MCUs) were introduced in the 1970s, combining processing, memory, and peripherals for electronic control. Initially dominated by 8-bit systems, they are widely used in applications like calculators and communication devices. Today, advanced 16/32-bit MCUs support a broad range of complex applications [1–6]. Digital transformation in dental radiology began in 1987 with the introduction of charge-coupled device systems. Other inventions like complementary metal oxide semiconductor and photo-stimulated phosphor (PSP) imaging systems enabled daylight operability of the devices, unlike film-based imaging that requires a dark room for film processing. Each digital imaging technology introduced distinct features, gradually improving efficiency and image quality in dental practice [7, 8].

In the photostimulable light mechanism, X-ray energy interacts with the BaFBr:Eu²⁺ or equivalent material, and electrons in the valence band are shifted to the conduction band, forming electron-hole pairs. When the stored energy is excited by electromagnetic energy of the proper spectrum, an illumination event occurs as electrons are transferred to Eu⁺³, releasing the stored energy. Inside a PSP scanner, the plate is excited pixel by pixel using the light source and the flying-spot rotating mirror. A photo-multiplier tube (PMT) with a filter to block the excitation light and only pass the photostimulable light spectrum acquires the light inside the device and transmits the signal through the analog-to-digital converter. The registered signal is processed to define the pixel gray values, resulting in the digital radiographic image [9]. Once a PSP plate is irradiated, the natural decay process begins slowly, and excessive ambient light exposure can accelerate the release of the energy stored in the plate, resulting in decreased signal quality on read-out [10, 11].

Corresponding author:

Hakan Amasya

E-mail:

hakanamasya@iuc.edu.tr or h-amasya@hotmail.com

Received: August 27, 2024

Revision Requested: November 19, 2024

Last Revision Received: January 6, 2025

Accepted: February 14, 2025

Publication Date: March 25, 2025

DOI: 10.5152/electrica.2025.24116



Content of this journal is licensed under a Creative Commons Attribution-NonCommercial 4.0 International License.

II. RELATED WORK

An early paper investigated the natural fading of the image signals, repeated scanning, and the light exposure required to erase the plates with the commercially available PSP plates from Fuji and Kodak and a scanner system that allows adjusting the PMT voltage, pre-digitization gain, image size to be scanned, and numerous other parameters. The latent image signals were found to decay very rapidly during the first several minutes and stabilize after several hours. Also, the different decay curves obtained in repeated experiments are consistent with the suggestion that different energy levels are required to excite the energy trapped in storage phosphor plates. The authors suggested that for quantitative measurements, the energy stored in the phosphor plates should be equilibrated for up to 2 hours, but the limitation of implementing this suggestion in clinical conditions was also mentioned [10].

A decade later, another study investigated the effect of visible light exposure on the irradiated PSP plates. The research was conducted with three types of light sources—cool white fluorescent tubes, aquarium fluorescent tubes, and incandescent filament bulb lamps—with three different light intensities—bright light at 10000 lx, well-lit office environment at 600 lx, and 20 lx dim light conditions. The results of this study supported the linearity in the dose response of the PSP plates; however, the erasure process was not proportionally linear with the total light output calculated as the product of light intensity and exposure time. The author mentioned that the results of this study were consistent with previous studies regarding multiple electron energy levels decay processes, and consequently, a high-order kinetics in the physical model of PSPs. The practical implication of this is that while a high rate of data loss is observed in the first few minutes of ambient light exposure of storage PSPs, the rate of energy loss decreases over time, and towards the end, excessive exposure is required to erase all of the remaining energy. Moreover, minor differences in the effectiveness of erasure were reported for various types of light sources [12].

Another study investigated the impact of ambient lighting intensity and duration on the signal-to-noise (SNR) using DenOptix and ScanX PSP systems. The study was conducted with different X-ray exposure times: 0.10 s, 0.20 s, and 0.32 s; ambient light intensity: 300 lx, 150 lx, and 20 lx; and a time range from <10 s to 120 s settings. The SNR was calculated by subtracting the “mean pixel value/standard deviation” from 255. The authors found that quality loss over time was greater at 300 lx light intensity than at 20 lx light intensity. At high light intensities, the effect of variation in SNR due to the amount of X-ray applied was found to be minor, whereas at lower light intensities, the resistance to image degradation was found to increase as the amount of X-ray applied to the plate increased. However, it was also emphasized that it is not good clinical practice to administer higher amounts of X-rays to patients to reduce image degradation due to ambient light [13].

In another research, the effect of the duration of ambient light exposure using two PSP-based systems was investigated quantitatively. The study was conducted with various X-ray exposure times: 0.10 s, 0.20 s, 0.32 s, 0.40 s, and 0.50 s, and durations of ambient light as 5 s, 10 s, 30 s, 60 s, and 90 s. Ambient light intensity was fixed at 80 lx, and half of the active surface of the imaging plate was covered from visible light exposure to test the effect of software restoration, and 18 ROIs were selected in each image for the quality tests. The resulting images were evaluated with five metrics: SNR, Contrast-to-noise

(CNR), brightness, contrast, and image saturation. Signal-to-noise values was calculated by dividing the mean gray value (MGV) of each ROI by the standard deviation, while the CNR was calculated by dividing the difference of MGV in adjacent steps by the average of the standard deviations of the two. Their experiment found a direct correlation between ambient light and the negative effect, with increasing light exposure leading to a decrease in SNR and CNR [14].

In previous studies, delayed scanning time or ambient light exposure was investigated only in static experiments with different light intensities or colors. In such experiments, which are usually performed with the same light source, it is possible to say that the standardization among experiments decreases when different colors and light sources are used. This pointed to the need for a tool that facilitates the reproduction of different light conditions. As a prototype, an Arduino-based embedded platform was designed and produced with additive manufacturing technology to experiment with the effect of light in Red-Green-Blue (RGB) colors using light-emitting diode (LED) light sources (Fig. 1 and 2). The system was based on an ATmega2560 8-bit microchip connected to TSL2591 and DHT11 sensors and LED outputs. A light-tight platform was produced with additive manufacturing, and the electronic parts were embedded into this platform. Thus, an experimental tool was developed that runs by reloading the code appropriate to the desired sequence (Fig. 3) [15, 16].

In the first study with this custom tool, the light intensity was calibrated according to full duty cycle (PWM) and ground illuminance (LUX), and light was applied for 1, 3, 5, and 10 minutes. For PWM calibration, signal loss was found to be higher in blue color most times, however, exposure to green light for 10 minutes resulted in a half-image. For PWM calibration, signal loss was found to be slower compared to the remaining colors, and the contrast loss was also slower. In that study, only one color of light was produced during each experiment, and different colors of light were not switched within the same sequence. In the experiment, the RGB LED source was tested to light the lamps according to the data coming from the optical illumination sensor on the floor, based on the fact that the light output power of the RGB LED source may be different for different colors. This calibration to the human eye showed that when LUX was fixed, green light was found to be safest for the energy stored in the PSP plate [15].

In the next study, three colors of light were sequentially turned on in the same order, and the effect of changing the sequence on quantitative image tests was examined. For this, possible combinations were tested at 20-second intervals in the first six experiments, while in the next six experiments, two different cycling patterns were tested at 1 s, 100 ms and 10 ms time intervals for a total of 1 minute. In that study, the highest SNR value was obtained in the Blue-Green-Red sequence and the lowest in the RGB sequence for the 20 s time interval experiments. Cycle experiments revealed an inverse relationship between SNR and time interval. The lowest CNR value among all experiments was found in the RGB sequence. In this early research, all three colors were turned on for the same amount of time in each experiment so that the total amount of light output was the same [16].

The first study [15] with this custom tool aimed to answer the question of which color light can be used in PSP scanning rooms to reduce the effect of ambient light. In the second study [16], the total light output was kept the same while the color was modulated during the

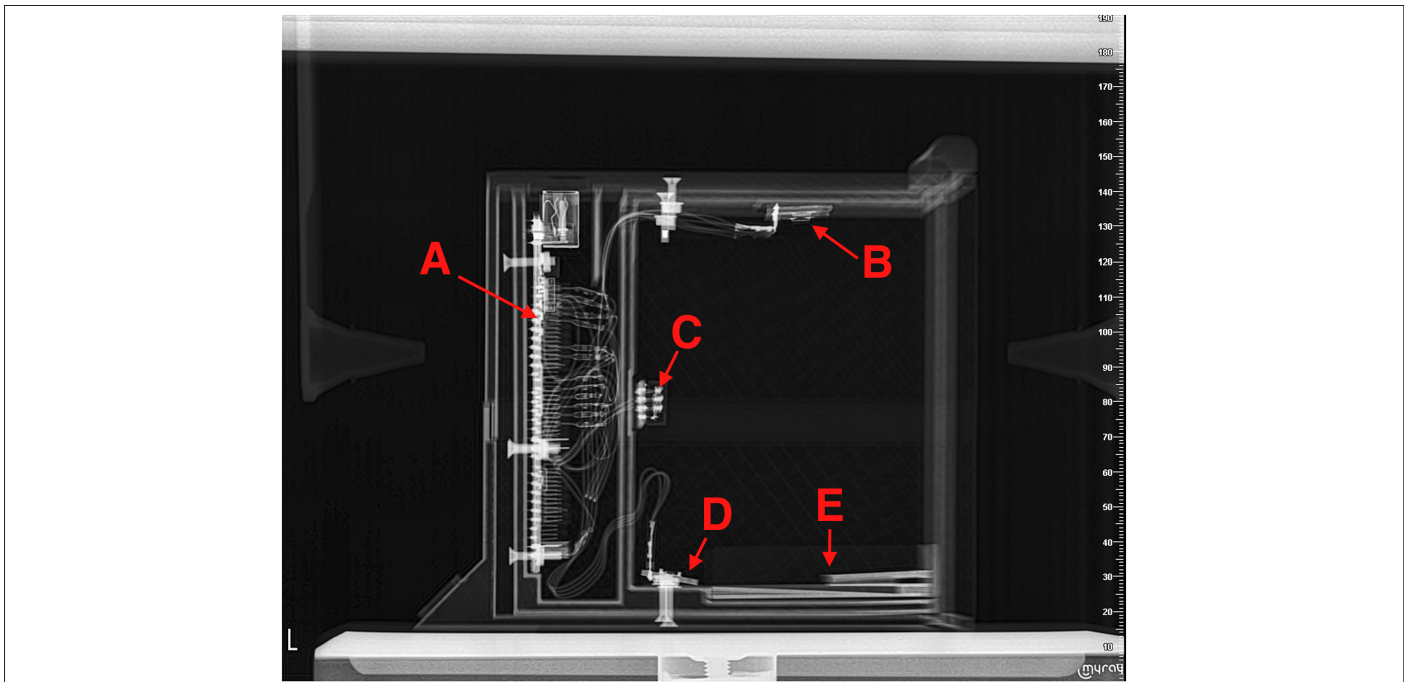


Fig. 1. The lateral x-ray image of the experimental tool demonstrating: A: Arduino Mega 2560 developer board, B: Red-Green-Blue Light-Emitting Diode light outputs, C: DHT-11 temperature and humidity sensor, D: TSL2591 high dynamic range digital light sensor, E: Mobile transport piece protecting half of the active surface.

experiment to test for variations. Studies have reported that the loss of stored energy in PSP plates is faster in the first few minutes and then begins to slow down until it becomes more stable [10–12]. This study aims to investigate the effect of applying the same amount of

light at different times within a 4-minute period, when signal loss is rapid in irradiated plates, and compare the effect on the final image quality by quantitative tests. For this purpose, continuous light was applied at the beginning, middle, and end of the delay period in three

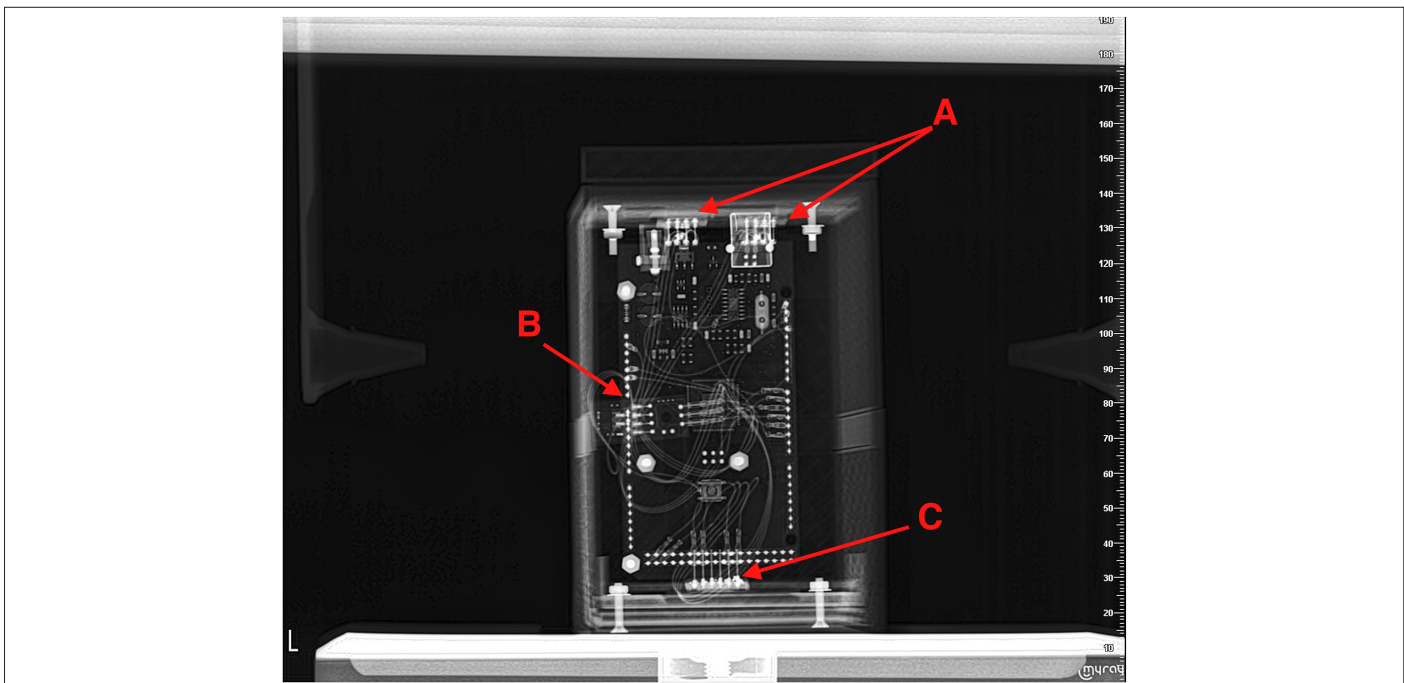


Fig. 2. The frontal x-ray view of the experimental tool demonstrates the internal electronic parts, in which A: RGB LEDs are located on the top, B: A humidity and temperature sensor is located on the wall, superimposed over the developer board, and C: A light sensor positioned on the floor.

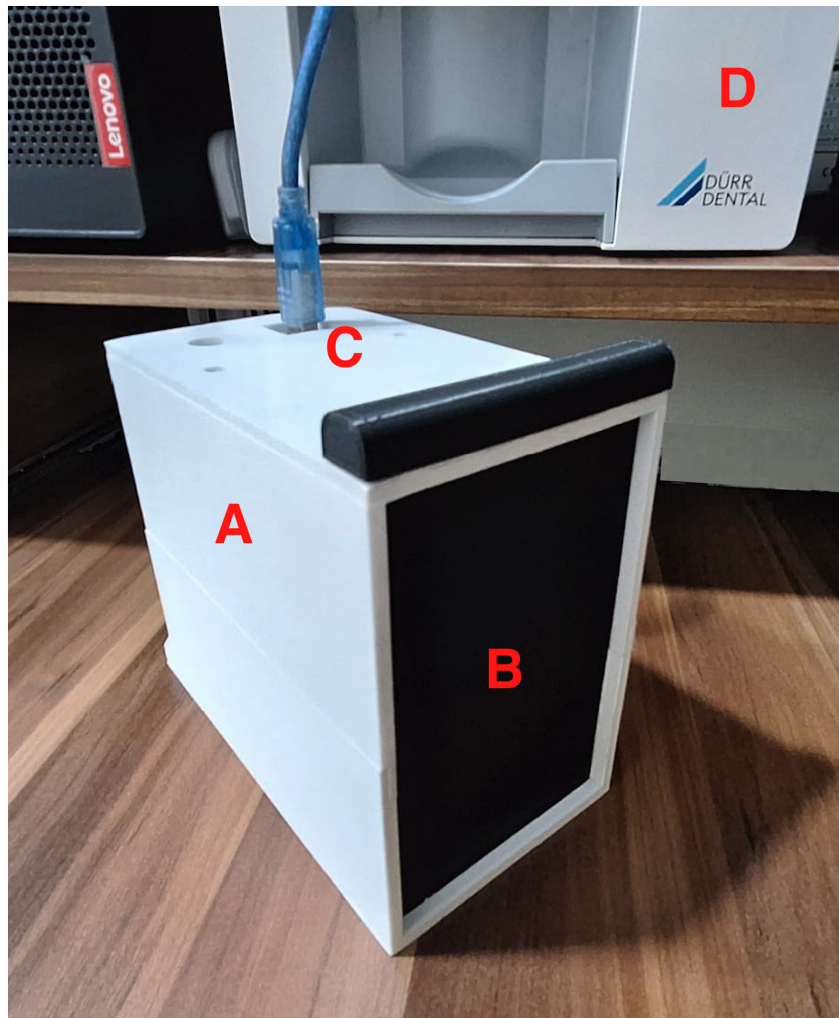


Fig. 3. A: Exterior view of the experimental tool after the assembly of all parts. B: The front black door is opened and closed manually, and the imaging plate is placed on the floor with the mechanical carrier piece. C: The device was powered and the data was transferred through a universal serial bus port. D: PSP scanning device used in this study.

different experiments, while interrupted light was applied at different time intervals in the remaining three experiments, and SNR and CNR values were calculated and compared in the digital images obtained.

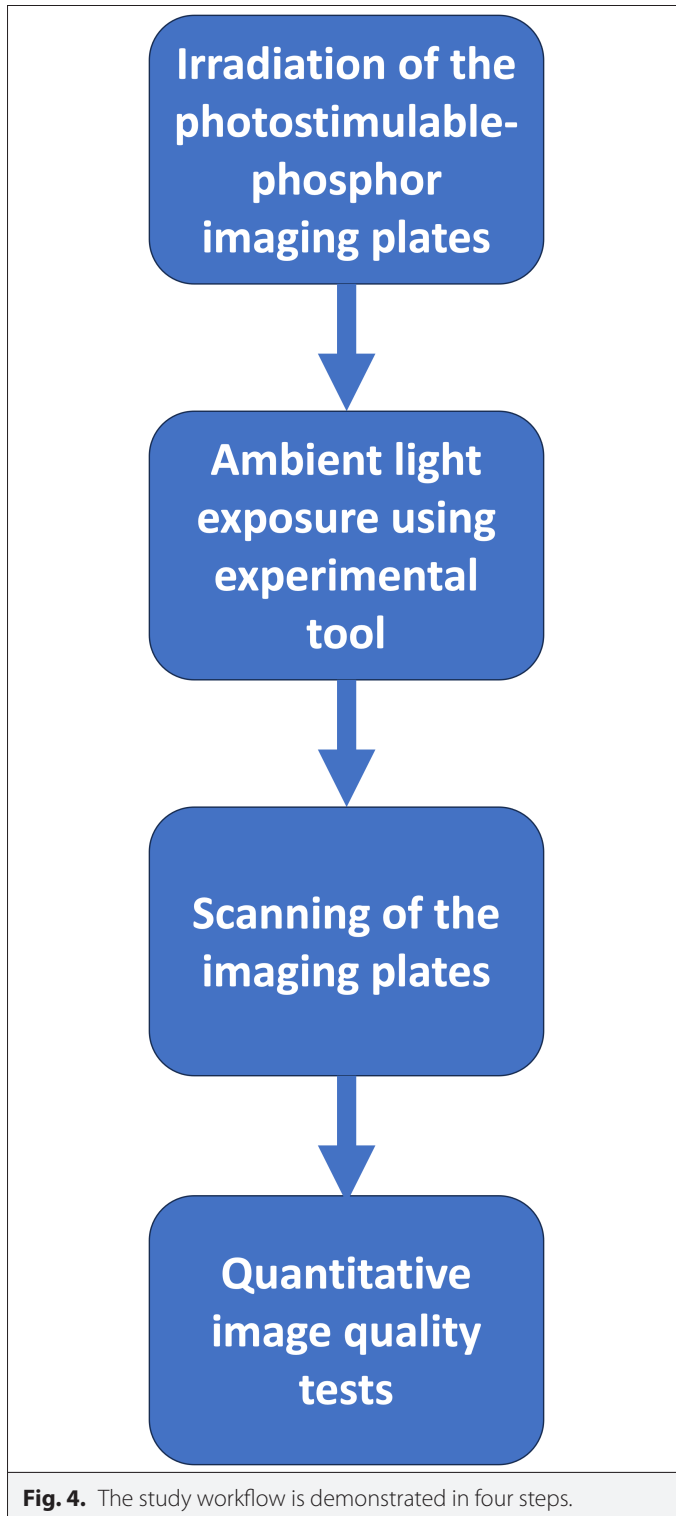
III. METHODOLOGY

In this study, the custom tool developed to study the effect of ambient lighting on PSP plate imaging [15, 16] was recoded and experiments were repeated using the custom-made aluminum step wedge. The study workflow is shown in Fig. 4.

A. Designing the Software

A new code was developed using the Arduino programming language. <Wire.h> was used to establish communication through the I2C protocol. <Adafruit_Sensor.h> provided a consistent framework for interfacing with and retrieving data from sensors, while <Adafruit_TSL2591.h> was used to store the state and functions of the TSL2591 Light Sensor, and <DHT11.h> was used to read temperature and humidity data from the DHT11 sensor. The TSL2591 ambient light sensor was operated with medium gain (25x) and an integration time of 300 ms. The data from the 16-bit sensor was

collected and processed with the 8-bit microcontroller using the bit shift function. The CH0 diode in the optical sensor registered the full spectrum (visible + infrared) of light, while the CH1 diode registered only the infrared spectrum. Thus, by subtracting the latter value from the first, visible light was obtained and this value was used to calculate the Lux, according to the algorithm in the library. The Lux, ambient temperature, and humidity values were periodically monitored on the serial port screen during the experiment. Input units were used to monitor the situation inside the sealed platform. None of the sensors were calibrated with an industry-grade counterpart after delivery. Since the system was designed to be static and not interactive, the sensor data was used only for monitoring the ambient conditions and did not trigger any action. For light generation, both LEDs were switched on simultaneously, and pseudo-white color was obtained by operating all three red, green, and blue colors at full duty cycle. Two different modes were determined for the on/off state of the LED light sources. In continuous mode, the light was switched on for 30 seconds and then switched off. In Interrupted mode, the light on/off state is cycled by changing according to the following time intervals: 5–15 s, 1–3 s, and 250–750 ms. Each sketch used 4%



of the total program storage space. Global variables used 7% of the dynamic memory, leaving the rest for local variables. The code was imported to the board using the Arduino Integrated Development Environment.

B. Processing of the Photo-Stimulated Phosphor Plates

Radiographic images were acquired using an RXDC (MyRay, Italy) intraoral X-ray source, 3 × 4 cm PSP plates (Dürr Dental, Germany),

and a VistaScan Mini Plus (Dürr Dental, Germany) scanner. A custom-made step-wedge measuring 2 × 2 × 1 cm was used to induce the contrast zones in radiographs. The contrast material was designed as a 5-step wedge and produced by milling an aluminum block with computer numerical control technology. The imaging plates were placed in hygienic covers, with the active surfaces covered by the black side of the cover. The step-wedge was positioned between the active surface and the X-ray source, with a fixed distance of 30 cm and imaging parameters of 70 kV, 8 mA, and 0.5 seconds of imaging parameters. The irradiated plate was taken to the mobile transport piece to be located on the platform, and half of the active surface was protected from the ambient light using a visor on the piece (Fig. 5). In all experiments, a total of 4 minutes were delayed between X-ray exposure and plate scanning. During this period, the first and last minute were allocated for transportation operations between the X-ray, tool, and scanner. For the remaining 2 minutes, a total of 30 seconds of full power light was emitted, and the light was off for the rest of the time, consistent across all six different experimental conditions in the study. Accordingly, 30 seconds of continuous light was emitted for the first three experiments, while in the remaining sequences, the light was switched on and off at a ratio of 1:3 at different time intervals over a 2-minute period (Fig. 6). The timeline of light exposures for the six distinct experiments in the study is shown in Fig. 7. This schedule is restricted to the 2-minute period during which light was delivered. At the end of 4 minutes after the application of LED-generated light, the plates were fed into the scanner with a theoretical spatial resolution of 40 lp/mm, and planar images were acquired using the scanner's built-in laser with a 635 nm wavelength, 10 mW output. Three repetitions were performed for each experimental condition. Six different setups were repeated for three times each, making a total of 18 images. The obtained radiographs were exported in .TIFF format for the quantitative image quality tests.

C. Quantitative Image Quality Tests

Image files are imported to the ImageJ software, and a total of 18 circular region of interests (ROIs) with a diameter of 1 unit were selected on each radiograph. Three ROIs were selected from the background, second and fourth steps of the step-wedge, separately for the dark side and the light side, and combined (Fig. 8). For the quantitative image quality measurements, bone and soft-tissue values were chosen as the second and the fourth steps of the step-wedge. Signal-to-noise and CNR values are calculated according to the given formulas in ref.[16].

$$SNR = \frac{\text{mean}(\text{bone})}{SD(\text{soft tissue})} \quad (1)$$

$$CNR = \frac{\text{mean}(\text{bone}) - \text{mean}(\text{soft tissue})}{SD(\text{soft tissue})} \quad (2)$$

D. Statistical Analysis

The distribution of the calculated values was evaluated with the Shapiro-Wilk test, and non-parametric tests were performed. The Kruskal-Wallis test and Wilcoxon signed-rank test were used to evaluate the independent and dependent variables, respectively. The Mann-Whitney *U* test was used to evaluate two-related samples. Kendall's Tau-b was calculated to measure the association between variables. The statistically significant threshold was determined as $p \leq 0.05$.

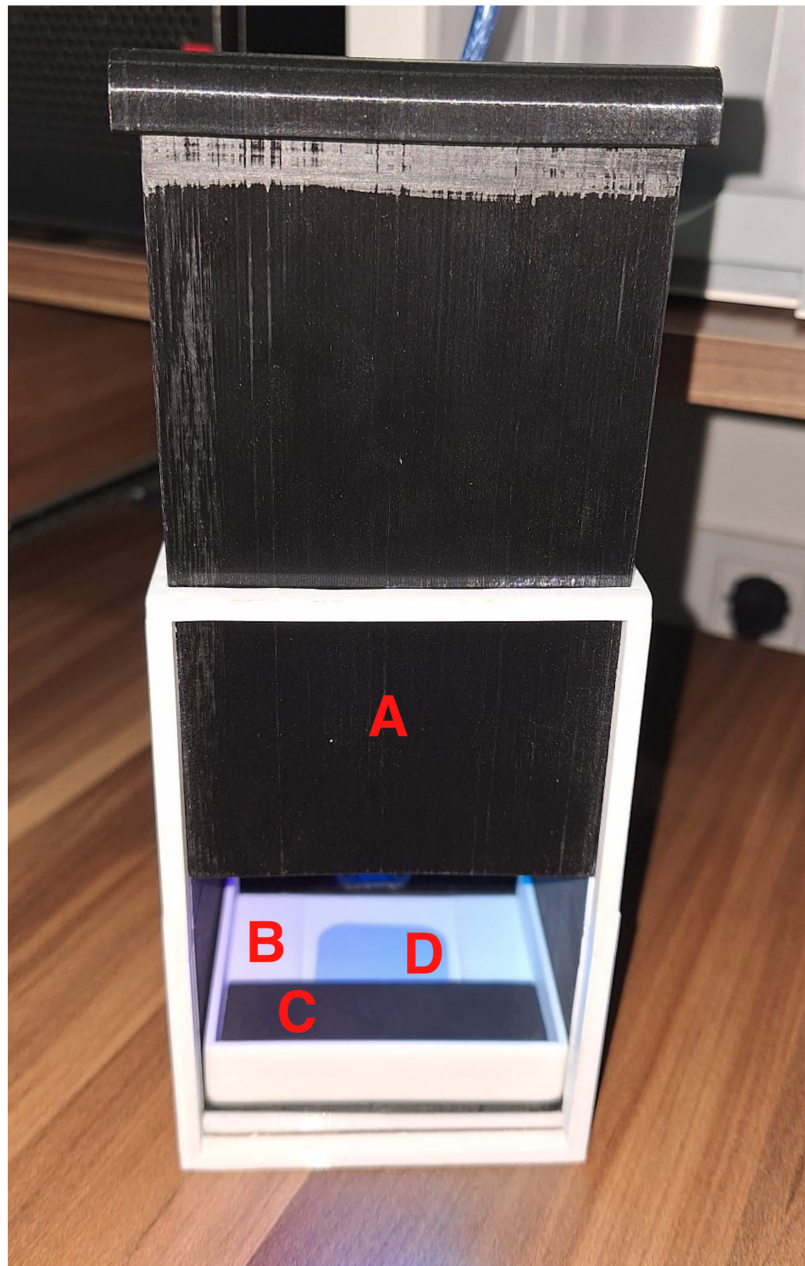


Fig. 5. Front cover open view of the experimental tool. A: Manual cover, B: Mobile transport part, C: Barrier protecting half of the imaging plate from light, D: Half of the active surface of the imaging plate.

IV. RESULTS

Sensor readings showed that the mean luminance inside the box was 177.72 ± 0.62 Lux in continuous experiments and 184.51 ± 0.08 Lux in interrupted experiments. As the sensor readings indicate that the temperature and humidity were stable inside the box, the temperature was recorded at 32°C and the humidity at 50%.

The SNR and CNR values for each condition are shown in Table I. Normality was tested with the Shapiro–Wilk test, and distribution of the SNR and CNR values in the first ($p=0.06$), fifth ($p=0.08$), and sixth ($p=0.43$) experiments, and the remaining experiments were not normally distributed ($p \leq 0.05$). When the data was split for the dark and

light sides, the results obtained in all experiments were found to be normally distributed ($p > 0.05$). Nevertheless, only non-parametric tests were conducted because the assumptions required for parametric tests were not met. According to the Wilcoxon signed-rank test, the comparison of SNR and CNR values for each experiment in light and dark regions was statistically significant ($p=0.03$). Also, light and dark side comparisons were statistically significant for both all ($p=0.02$) and SNR and CNR ($p=0.028$) values.

As the dark and light-side were split, the Kruskal–Wallis test showed that comparing the differences in three repetitions for each experiment was not statistically significant ($p > 0.05$). A comparison of the results of the continuous experiments with each other and the

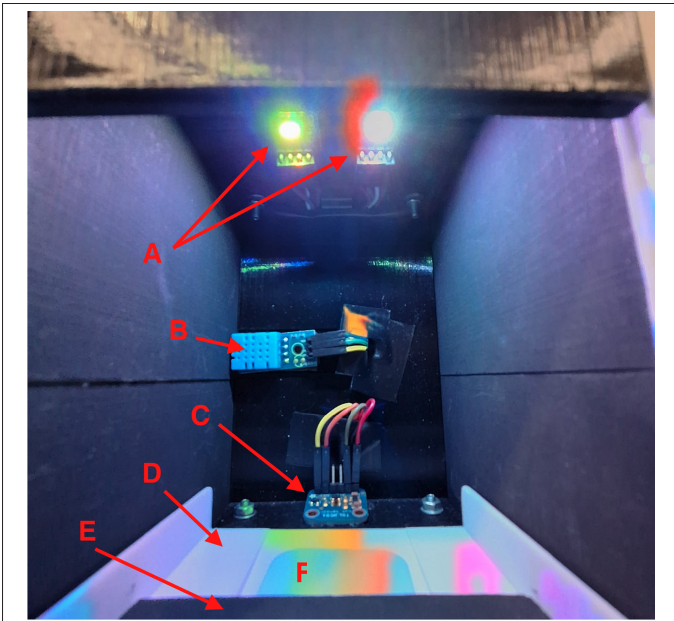


Fig. 6. Internal view of the experimental tool. A: RGB LEDs, B: DHT-11, C: TSL2591, D: Carrier platform, E: Light barrier, F: Imaging plate.

interrupted experiments with each other was found to be statistically insignificant ($p > 0.05$). Mann-Whitney U test suggested that comparing the values on the dark side was statistically significant ($p=0.046$), while it was not significant ($p=0.369$) on the light side of the plate.

Kendall's Tau-b test showed a significant correlation between the SNR or CNR tests and the calculated values ($p < 0.01$). If the dark and light sides are divided, in the former, in the interrupted mode, there was a significant correlation between the calculated values and the number of experiments ($p=0.029$) and repetitions ($p=0.043$), while the relationship between test and values was not significant ($p=0.070$). On the light side, there was a significant ($p < 0.01$) correlation between test and values for both continuous and interrupted modes.

Accordingly, on the dark side, the lowest mean SNR (124.1) and CNR (76.6) were found in Experiment 2, and the highest in Experiment 6

(SNR: 247.8, CNR: 154.6). The mean SNR and CNR values were found to be 156.4 and 88.7 in continuous type experiments and 193.1 and 119.2 in interrupted experiments, respectively (Fig. 9). On the light side, the lowest SNR (257.4) and CNR (23.7) values were found in Experiment 5, while the highest values were observed in Experiment 4 for SNR (440.4) and Experiment 2 for CNR (46.7). The average SNR and CNR values were 376.4 and 42.7 for continuous experiments and 377.5 and 33.5 for interrupted experiments, respectively (Fig. 10).

V. DISCUSSION

In this research, an Arduino-based tool developed to investigate the effect of ambient light between irradiation and scanning in a PSP imaging system was reprogrammed, and the effect on quantitative image quality test results was investigated by changing the timing of light production under fixed total delay and light output conditions. Although some differences in SNR and CNR values were observed in the experiments with continuous and interrupted light, they were mostly statistically insignificant.

The effect of ambient light on phosphor plates was investigated in previous studies using various methods. Developing an Arduino-based system requires relatively simple training in hardware and software, allowing researchers to produce the prototypes they consider. In this study, no soldering was performed, and all connections were made with jumper cables. Moreover, open-access libraries were used as software, and a simple algorithm was developed without any formal training in the field. This was an opportunity for someone from outside the electronics field to develop a tool to address the problem, thanks to the Arduino project. Additionally, additive manufacturing was used to build the platform, and the milling technique was adopted in step-wedge production. Thus, custom tools were designed and manufactured to be used in this research.

The main motivation for this study was the theory that energy stored in the PSP plates is captured and released at different stages. However, in related studies, it is mentioned that the energy stored in phosphor plates fades mostly in the first few minutes, and the energy stored in the plates only stabilizes after a few hours [10–12]. Although it is recommended to wait a few hours for the stabilization of phosphor plates for quantitative measurements, in this study, the time taken before X-ray application and scanning was fixed at 4 minutes. This is close to the time required for imaging in a clinic.

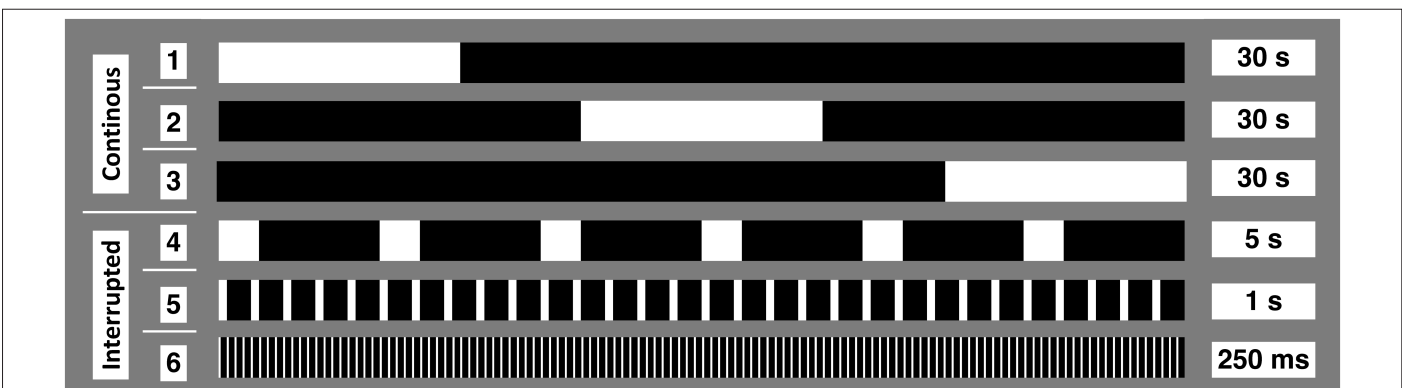


Fig. 7. Timeline of the sequences conducted in this study. Only pseudo-white color was used, and the LEDs were turned on and off according to the scheme. The white areas in this timeline represent when the LEDs are on, and the black areas represent when they are off.

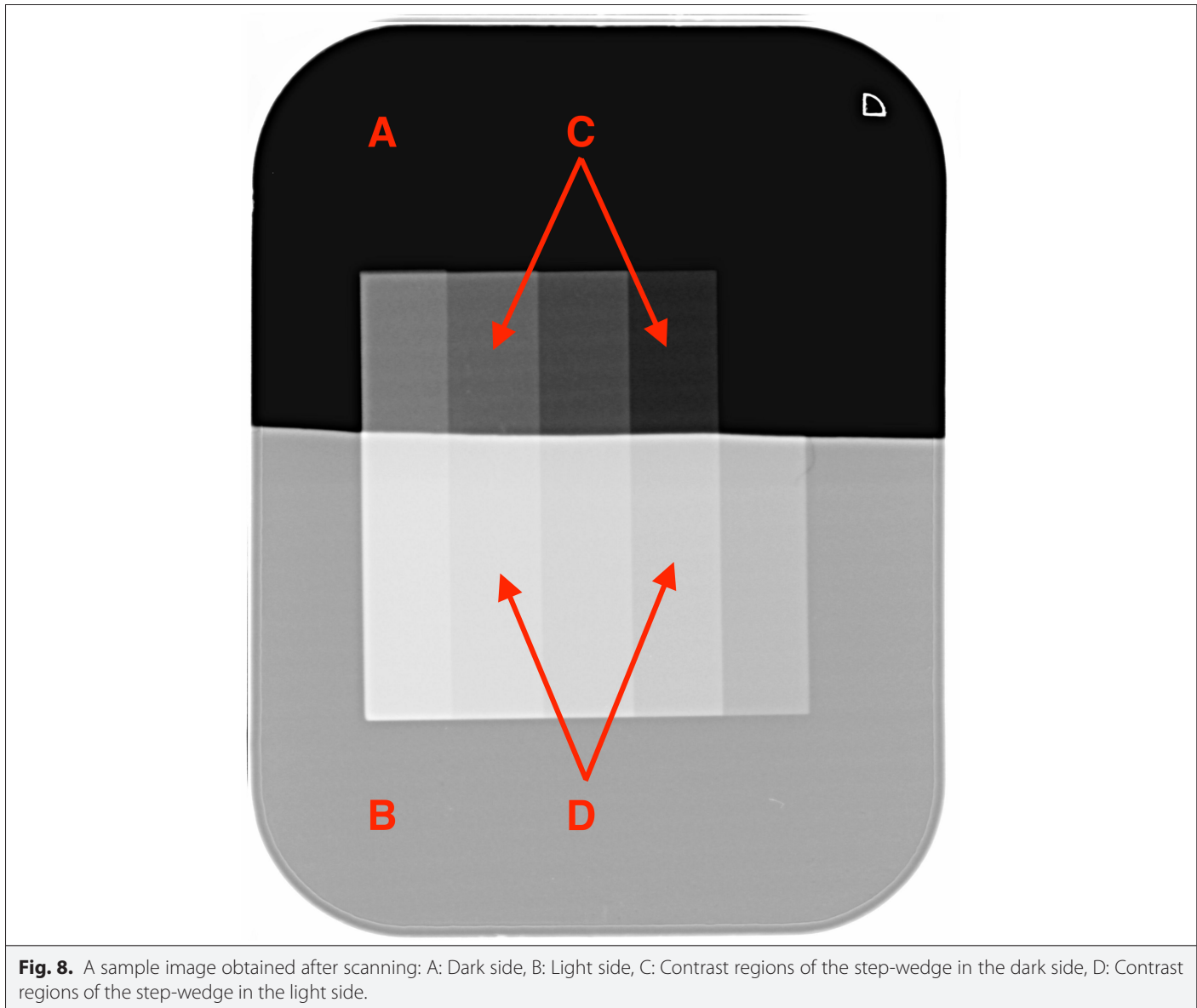


Fig. 8. A sample image obtained after scanning: A: Dark side, B: Light side, C: Contrast regions of the step-wedge in the dark side, D: Contrast regions of the step-wedge in the light side.

However, the first and last minutes of this time were reserved for the handling of the plate, and no light was applied during this time. In the 2 minutes in between, light was projected at different time periods.

The sensors used to monitor environmental changes (illumination, temperature, and humidity) inside the sealed box during the experiments were not calibrated before the experiment using industry-grade equipment. Although there may be tolerable errors in the calculated values in the respective units, this is not an obstacle to monitoring changes in ambient conditions. Nevertheless, it is important to remember the importance of sensor calibration for more accurate measurements.

Photo-stimulated phosphor systems offer a wide dynamic range but also record unwanted photons, such as secondary or backscatter radiation. Image production software may compensate for such photons outside the desired energy level and restore any potential signal loss due to delayed scanning time or ambient light. However,

once the extreme deviations are removed, the smallest and largest signals are assigned to the boundaries of the 8-bit pixel value (0–255), while the rest are assigned to the corresponding values. Half of the active surfaces of the phosphor plates were therefore protected from the light treatment. Thus, the change in the light side of the plate indicates the loss of signal after light exposure, and the change in the dark side may indicate the effect of compensating for this loss. The evaluation of image restoration algorithms on diagnostic objectives is beyond the scope of this study [17–19].

According to the results, in continuous experiments, the production of light in the middle of the delay period (Experiment 2) resulted in the highest image quality on the light side (SNR: 412, CNR: 46.7) and the lowest on the dark side (SNR: 124.1, CNR: 76.6). Comparing dark and light-sides ($p=0.02$) may support the suggestion that the restoration of signal loss also affects the parts of the plate that is not affected by signal loss. In the interrupted experiments, a non-monotonic relationship was observed on the light-applied side, while a monotonic graph was observed on the dark side. When evaluating

TABLE I. QUANTITATIVE IMAGE QUALITY TEST RESULTS AS SNR AND CNR VALUES FOR DARK AND LIGHT SIDES, EXPERIMENTS, AND REPETITION ARE GIVEN AS THE CONTINUOUS AND INTERRUPTED TYPES ($P \leq 0.05$).

Type	Experiment	Repetition	Dark Side			Light Side				
			SNR	CNR	p_1	SNR	CNR	p_1	p_1	
Continuous	1	1	147.2	89.7	0.028*	245.3	28.1	0.028*	0.020*	
		2	212.0	132.2		524.5	59.3			
		3	205.0	56.9		301.7	34.4			
		p_2	0.651			0.565				
	2	1	133.7	81.5	0.028*	245.2	28.4	0.028*	0.020*	
		2	139.3	86.4		406.3	45.9			
		3	99.1	61.9		584.4	65.8			
		p_2	0.565			0.565				
	3	1	124.0	76.2	0.028*	312.7	35.5	0.028*	0.020*	
		2	203.5	124.0		197.1	22.9			
		3	143.4	89.3		569.9	63.9			
		p_2	0.399			0.565				
		p_2	0.399			0.895				
	Interrupted	4	1	98.0	60.6	0.028*	701.0	68.6	0.028*	0.020*
			2	153.7	92.7		257.6	25.8		
3			213.1	128.7	362.6		35.7			
		p_2	0.276			0.565				
5		1	113.7	68.5	0.028*	289.3	27.0	0.028*	0.020*	
		2	115.3	69.3		302.1	27.2			
		3	300.7	189.2		180.7	16.9			
		p_2	0.156			0.565				
6		1	310.6	195.6	0.028*	364.4	29.3	0.028*	0.020*	
		2	213.4	131.2		544.3	40.4			
		3	219.4	137.1		395.1	30.5			
		p_2	0.565			0.565				
		p_2	0.135			0.337				
		p_3	0.046*			0.369				

p_1 : Wilcoxon signed rank test, p_2 : Kruskal-Wallis test, p_3 : Mann-Whitney U test, SNR: Signal-to-noise, CNR: Contrast-to-noise.

* Statistically significant at $p \leq 0.05$ (2-tailed).

the results of the study, it should be kept in mind that there may be method errors, the suggestion of different energy levels in the phosphor plates, and the effect of restoration software on the obtained values.

In the present study, the recommended stabilization time of 1–2 hours for quantitative measurements with the PSP system was not reached, and the measurements were limited to the first few minutes when signal loss was the most rapid. Although this is consistent with

the time required in the clinic, it can be considered a limitation of the study. In planning future work, it may be useful to consider the topics independently. For example, for the X-ray source, different kVp, mAs, and source-object distances could be tested. For the PSP system, other brands of imaging plates, scanner devices, and software could be tested. Different experiments can be designed concerning the time after irradiation and before scanning, ambient lighting, temperature, humidity, and other parameters. For quantitative image quality tests, fully automatic algorithms can be developed instead of manual

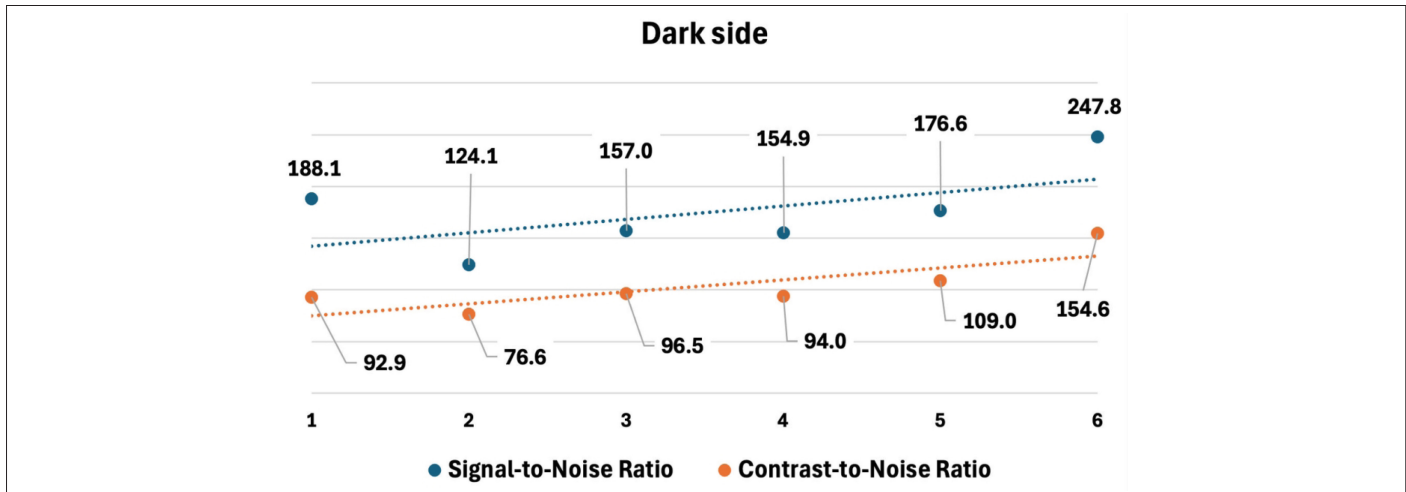


Fig. 9. Average signal-to-noise and contrast-to-noise ratio values calculated from step-wedge steps on the dark side of the image.

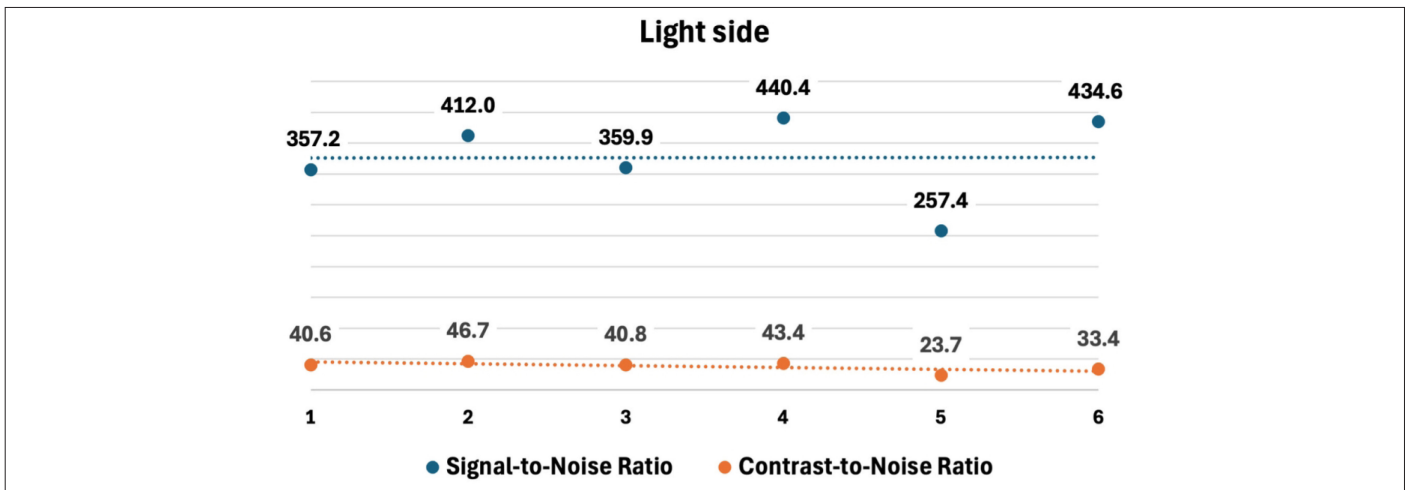


Fig. 10. Average signal-to-noise and contrast-to-noise ratio values calculated from step-wedge steps on the light side of the image.

ROI selection. In the improvement of the current experimental tool, different sensors can be added to increase the machine's environmental awareness, and manual processes can be replaced with automatic moving components. The necessary features for this system to work independently from the computer can also be considered.

VI. CONCLUSION

In this study, the effect of timing of ambient light exposure on PSP plates prior to scanning was investigated. For this purpose, six different experiments were repeated three times, however, the ambient light exposure was limited to the first few minutes when signal loss was most intense. While differences were found in quantitative image quality tests, the majority of these differences were not statistically significant. Results of the second experiment may support the suggestion that the restoration of signal loss also affects the parts of the plate that is not affected by signal loss. Further investigation may be performed with longer delay times and an advanced tool that offers more standardized repetition. In further research, longer delay times can be studied, where the energy stored in phosphor plates is more stable.

Availability of Data and Materials: The data that support the findings of this study are available on request from the corresponding author.

Acknowledgment: The 3D printed platform was designed, produced, and combined in the Cerrahpaşa Research, Simulation and Design Center (CAST).

Peer-review: Externally peer-reviewed.

Declaration of Interests: The author has no conflict of interest to declare.

Funding: The author declared that this study has received no financial support.

REFERENCES

1. K. R. Raghunathan, "History of microcontrollers: First 50 years", *IEEE Micro*, vol. 41, no. 6, pp. 97–104, 2021. [\[CrossRef\]](#)
2. F. Faggin, "How we made the microprocessor", *Nat. Electron.*, vol. 1, no. 1, pp. 88–88, 2018. [\[CrossRef\]](#)
3. K. Shirriff, "The surprising story of the first microprocessors", *IEEE Spec.*, vol. 53, no. 9, pp. 48–54, 2016. [\[CrossRef\]](#)

4. M. K. Parai, B. Das, and G. Das, "An overview of microcontroller unit: from proper selection to specific application", *IJSCE*, vol. 2, no. 6, pp. 228–231, 2013.
5. D. E. Bolanakis, "A survey of research in microcontroller education", *IEEE R. Iberoamericana Tecnologias Aprendizaje*, vol. 14, no. 2, pp. 50–57, 2019. [\[CrossRef\]](#)
6. H. K. Kondaveeti, N. K. Kumaravelu, S. D. Vanambathina, S. E. Mathe, and S. Vappangi, "A systematic literature review on prototyping with Arduino: Applications, challenges, advantages, and limitations", *Comput. Sci. Rev.*, vol. 40, p. 100364, 2021. [\[CrossRef\]](#)
7. R. Pauwels, "History of dental radiography: Evolution of 2D and 3D imaging modalities", *Med Phys Int*, Vol. 8, no. 1, pp. 235–277, 2020.
8. M. H. Yoshida, H. Yoshihara, and E. Honda, "History of digital detectors in intraoral radiography", *Dent. Health Curr. Res.*, vol. 4, no. 2, 2018. [\[CrossRef\]](#)
9. P. Leblans, D. Vandenbroucke, and P. Willems, "Storage phosphors for medical imaging", *Materials (Basel)*, vol. 4, no. 6, pp. 1034–1086, 2011. [\[CrossRef\]](#)
10. C. Shaw, J. Herron, and D. Gur, "Signal fading, erasure, and rescan in storage phosphor imaging", in *J. Med. Imaging VI: Instrumentation*, R. Shaw, Ed. International Society for Optical Engineering, vol. 1651, Newport Beach, California: 1992, pp. 156–163.
11. G. W. Seeley, H. Roehrig, and W. J. Dallas, "Delayed readout of computed radiography receptor plates: Effects on perceived image quality", *Image Process.*, vol. 1092, pp. 367–373, 1989. [\[CrossRef\]](#)
12. R. Molteni, "Effect of visible light on photo-stimulated-phosphor imaging plates" *Int. Congr. S.*, vol. 1256, pp. 1199–1205, 2003. [\[CrossRef\]](#)
13. R. Ramamurthy, C. Canning, J. Scheetz, and A. Farman, "Impact of ambient lighting intensity and duration on the signal-to-noise ratio of images from photostimulable phosphor plates processed using DenOptix® and ScanX® systems", *Dento Maxillo Facial Rad.*, vol. 33, no. 5, pp. 307–311, 2004. [\[CrossRef\]](#)
14. M. Sampaio-Oliveira, L. E. Marinho-Vieira, V. A. Wanderley, G. M. B. Ambrosano, R. Pauwels, and M. L. Oliveira, "How does ambient light affect the image quality of phosphor plate digital radiography? A quantitative analysis using contemporary digital radiographic systems", *Sensors (Basel)*, vol. 22, no. 22, p. 8627, 2022. [\[CrossRef\]](#)
15. H. Amasya, K. Orhan, and A. Alkan, "Comparison of the effect of the time under the three primary color lighting of led production before scanning of phosphorus plates", *Eur. Ann. Dent. Sci.*, vol. 49, no. 3, pp. 131–138, 2022. [\[CrossRef\]](#)
16. I. Yel et al., "Optimization of image quality and radiation dose using different cone-beam CT exposure parameters", *Eur. J. Rad.*, vol. 116, pp. 68–75, 2019. [\[CrossRef\]](#)
17. M. Sampaio-Oliveira, L. E. Marinho-Vieira, M. Barros-Costa, and M. L. Oliveira, "Can digital enhancement restore the image quality of phosphor plate-based radiographs partially damaged by ambient light?", *J. Imaging Inform. Med.*, vol. 37, no. 1, pp. 145–150, 2024. [\[CrossRef\]](#)
18. M. Sampaio-Oliveira, L. E. Marinho-Vieira, F. Haiter-Neto, D. Q. Freitas, and M. L. Oliveira, "Ambient light exposure of photostimulable phosphor plates: Is there a safe limit for acceptable image quality?", *Dento Maxillo Facial Rad.*, vol. 52, no. 7, p. 20230174, 2023. [\[CrossRef\]](#)
19. H. Gaëta-Araujo, N. Oliveira-Santos, L. de Oliveira Reis, E. H. L. Nascimento, and C. Oliveira-Santos, "Automatic exposure compensation of digital radiographic technologies does not affect alveolar bone-level measurement", *Oral Rad.*, vol. 39, no. 1, pp. 53–58, 2023. [\[CrossRef\]](#)



Hakan Amasya was graduated from Ege University, Faculty of Dentistry in 2013. He completed his specialty training in Oral, Dental, and Maxillofacial Radiology at Süleyman Demirel University, Faculty of Dentistry in 2019. In late 2019, he started working at Tekirdağ Çorlu Oral and Dental Health Center as an Oral, Dental, and Maxillofacial Radiology Specialist and stayed there for about a year. In 2020, he began working as an assistant professor at İstanbul University-Cerrahpaşa, Faculty of Dentistry, and his position is still ongoing. Hakan Amasya, who studied radiographic bone age assessment with machine learning in his specialty thesis, currently conducts research on subjects such as computer-aided diagnosis and additive manufacturing.